

## Theoretical investigation of internal conversion in chromyl chloride

S RASHEV

Institute of Solid State Physics, Bulgarian Academy of Sciences, 1187 Sofia, Bulgaria

**Abstract.** The internal conversion process from single vibronic levels in the first excited electronic state  $S_1$  of chromyl chloride was theoretically investigated. On the basis of this analysis certain important features of the experimentally observed fluorescence decay from  $S_1$  have been understood. Implications of the obtained results to multiphoton chemistry are discussed.

**Keywords.** Chromyl chloride; internal conversion; intramolecular vibrational relaxation.

### 1. Introduction

Recently a novel method of multiphoton chemistry has been established, which is based on the “hot molecule” mechanism (Nakashima and Yoshihara 1989). Namely, after UV excitation into a higher molecular electronic state, internal conversion (IC) into the highly vibrationally excited ground electronic state ( $S^{**}$ ) occurs. This (hot) state shows absorption in the UV region, so it can absorb another photon and subsequently undergo dissociation (or some other type of monomolecular reaction). Of crucial importance for the characterization and optimization of this procedure would certainly be the investigation of the nature and dynamics of the vibrational distribution in the “hot” intermediate state  $S_0^{**}$ , which arises from the interplay of both IC and intramolecular vibrational relaxation (IVR). We have chosen as the object of our theoretical investigation the molecule chromyl chloride. We note that hitherto the multiphoton procedure described above has not been applied to chromyl chloride, but this molecule seems to be particularly suitable for such a treatment. On the other hand  $\text{CrCl}_2\text{O}_2$  is of special interest, as the fluorescence from single vibronic levels (SVL) of the  $S_1$  state has been shown to possess certain remarkable features, indicative of complicated relaxation behaviour in the excited state (McDonald 1975; Tinti *et al* 1989): biexponential fluorescence decays; steep (and mode-selective) decrease of fluorescence quantum yield (QY) with excess vibrational energy ( $E^{\text{vib}}$ ) in  $S_1$ .

### 2. Biexponential fluorescence decay

The origin of  $S_1(B_1)$  is at  $17,248\text{ cm}^{-1}$ . Biexponential fluorescence decay was observed (Tinti *et al* 1989) from several SVL, corresponding to varying excitation of the  $\nu_4$  mode:

$$S(t) = A_F \cdot \exp(-K_F t) + A_S \cdot \exp(-K_S t), \quad S(0) = 1, \quad (1)$$

$S(t)$  – fluorescence intensity;  $K_F, A_F$  – rate constant and amplitude of fast decay;  $K_S, A_S$  – rate constant and amplitude of slow decay ( $K_F > K_S; A_F/A_S \approx 1$ ).  $K_F$  and  $K_S$

substantially depend upon the number  $n'_4$  of excited  $\nu'_4$  ( $136\text{ cm}^{-1}$ ) quanta in  $S_1$ . The dependence, experimentally observed by Tinti *et al* (1989) is:  $K_F = K_F^0 \cdot \exp(\alpha_F \cdot n'_4)$ ,  $K_S = K_S^0 \cdot \exp(\alpha_S \cdot n'_4)$ , where  $\alpha_F = 1.06$ ;  $K_F^0 = 13.9$ ;  $\alpha_S = 1.45$ ;  $K_S^0 = 0.93$ . Both  $K_F$  and  $K_S$  grow with  $n'_4$ , but as  $K_S$  grows more steeply, their values get closer.

Fluorescence QY diminishes strongly with  $n'_4$  and practically no fluorescence results when exciting vibronic levels of  $S_1$  at  $E^{\text{vib}} > 600\text{ cm}^{-1}$ . Absorption of light with frequency above  $23800\text{ cm}^{-1}$  leads to dissociation of  $\text{CrCl}_2\text{O}_2$  by breaking the Cr-Cl bonds, leading finally to  $\text{CrO}_2 + \text{gaseous Cl}_2$  (Halonbrenner *et al* 1968).

### 3. Model

The (biexponential) fluorescence relaxation behaviour of  $S_1$  chromyl chloride could be explained by the following model (suggested by Tinti *et al* 1989). According to Lahmani *et al* (1974) the involvement of an intermediate state is necessary for biexponential decay to arise. The central point of the model (figure 1) is that the initially excited  $S_1$  vibronic level ( $\varphi_0$ ) decays nonradiatively (IC) to a sparse manifold of highly vibrationally excited  $S_0^{**}$  levels  $\varphi_1$ , distinguished by their comparatively large interaction matrix elements of  $\varphi_0$ . Those levels  $\varphi_1$  subsequently decay (through IVR) to the entire available isoenergetic vibronic level density  $\varphi'_1$ , belonging to  $S_0^{**}$ .

### 4. Kinetic description

The following equations, describing the situation in figure 1 can easily be derived:

$$K_{F,S} = \frac{1}{2}(K_{fl} + K_{IC} + K_{IVR} + K'_{IC}) \pm \frac{1}{2}[(K_{fl} + K_{IC} - K_{IVR} - K'_{IC})^2 + 4K_{IC}K'_{IC}]^{\frac{1}{2}}$$

$$A_F/A_S = (K_{fl} + K_{IC} - K_S)/(K_F - K_{fl} - K_{IC})$$

$$QY = K_{fl}(A_F/K_F + A_S/K_S). \quad (2)$$

Equation (2) gives the rate constants of the real decay processes involved –  $K_{fl}$ ,  $K_{IC}$ ,  $K'_{IC}$ ,

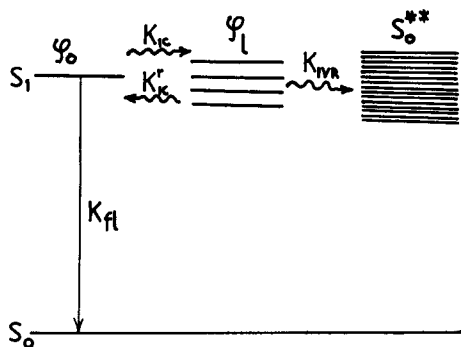


**Figure 1.** Schematic representation of the model employed for rationalizing the biexponential fluorescence delays from  $S_1$  – chromyl chloride;  $K_{IC}$ ,  $K'_{IC}$  – rate constants for direct and inverse internal conversion respectively;  $K_{IVR}$  – rate constant for IVR.

**Table 1.** Dependence of the quantities (specified below) on the number  $n'_4$  of excited  $\nu_4$  quanta in  $S_1$ ;  $K_{F,S}$ ,  $A_{F,S}$  – rate constants and amplitudes of fast and slow decay, respectively; QY – fluorescence quantum yield;  $K_{IC}$ ,  $K'_{IC}$  and  $K_{IVR}$  as in figure 1.

$n'_4$	$K_F(s^{-1})$	$K_S$	$A_F/A_S$	QY	$K_{IC}$	$K'_{IC}$	$K_{IVR}$
1	$4.0 \cdot 10^7$	$4.0 \cdot 10^6$	1.01	0.50	$1.8 \cdot 10^7$	$1.7 \cdot 10^7$	$4.3 \cdot 10^6$
2	$1.1 \cdot 10^8$	$1.7 \cdot 10^7$	1.10	0.50	$5.7 \cdot 10^7$	$4.2 \cdot 10^7$	$2.7 \cdot 10^7$
3	$3.3 \cdot 10^8$	$7.2 \cdot 10^7$	1.20	0.10	$1.8 \cdot 10^8$	$9.5 \cdot 10^7$	$1.2 \cdot 10^8$
4	$9.6 \cdot 10^8$	$3.1 \cdot 10^8$	8.00	0.01	$3.7 \cdot 10^8$	$1.1 \cdot 10^8$	$7.8 \cdot 10^8$

$K_{IVR}$  (figure 1) from the experimentally observed characteristics of the biexponential decay –  $K_F$ ,  $K_S$ ,  $A_F/A_S$ , QY, for each value of  $n'_4$ . Table 1 illustrates the results obtained.

## 5. Computation of IC rates

The central point of the present work is the estimation of  $\{\phi_i\}$  level densities and the magnitude of their coupling strength to  $\phi_0$ . Only a very schematic description of the computations will be presented below, a more detailed account being given elsewhere (Rashev 1991).

*Basic definitions* (Avouris *et al* 1977):

$$\phi_0 = \psi_{S_1}(r, Q) \cdot \phi_0(Q), \quad \phi_1 = \psi_{S_0}(r, Q) \cdot \phi_1(Q) \text{ – zero-order}$$

Born-Oppenheimer vibronic states.

$$V_{oi} = \langle \phi_0 | H | \phi_i \rangle \approx v_p/2 \langle \psi_{S_1} | \partial/\partial Q_p | \psi_{S_0} \rangle \langle \phi_0 | \partial/\partial Q_p | \phi_i \rangle \quad (3)$$

$H$  – molecular electronic-vibrational hamiltonian;  $v$ ,  $Q_p$  – frequency and coordinate of the main promoting mode of the IC process.

$$V_{oi}^{el} = v_p/2 \langle \psi_{S_1} | \partial/\partial Q_p | \psi_{S_0} \rangle \text{ – electronic factor,}$$

$$FC = \langle \phi_0 | \partial/\partial Q_p | \phi_i \rangle \text{ – Franck-Condon factor.}$$

The FC factor was computed under the following assumptions. The Cr–O stretch vibrations [ $\nu_1''(A_1) = 995 \text{ cm}^{-1}$  and  $\nu_6''(B_1) = 1002 \text{ cm}^{-1}$ ] are taken as one couple of local modes (Henry 1977), the Cr–Cl stretches [ $\nu_2''(A_1) = 475 \text{ cm}^{-1}$  and  $\nu_8''(B_2) = 500 \text{ cm}^{-1}$ ] form the second couple of local modes. The rest five vibrations of  $\text{CrCl}_2\text{O}_2$  are considered as normal modes.

For the local modes Morse oscillator formalism was applied. Basic parameters involved in the description are:  $Q_0$  – shifts of equilibrium position of the oscillator in electronic states  $S_0$  and  $S_1$ ;  $K = (v'/v'')^{1/2}$  – change of fundamental frequency;  $\omega x$  – anharmonicity parameter of the Morse oscillator.

For the normal modes harmonic oscillator formalism was applied. Here, only the  $Q_0$  – shift parameter was accounted for. The electronic factor  $V_{oi}^{el}$  was arbitrarily taken as  $10 \text{ cm}^{-1}$ . As a promoting mode the Cr–O stretch was employed. Thus, by

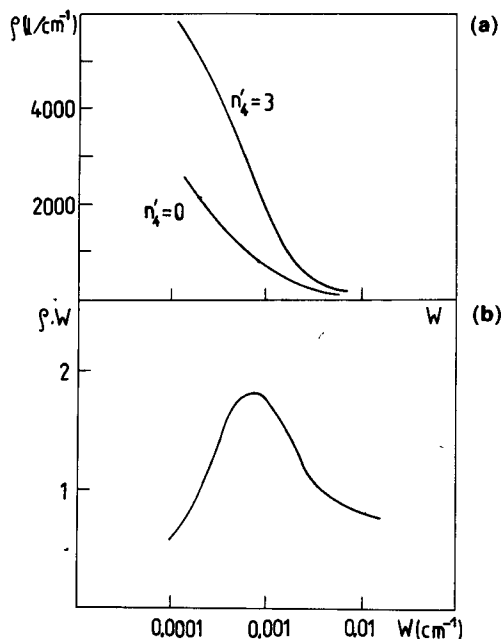


**Figure 2.** (a) Computed dependence of the density  $\rho(W)$  of vibronic levels which interact with the initial level  $\varphi_0$  through matrix elements exceeding  $W$ . (b) Presentation of the dependence  $W \cdot \rho(W)$  (discussed in the text).

adopting definite values for the above parameters, we are able to calculate the value of  $V_{0i}$  for any couple of zero-order states  $\varphi_0$  and  $\varphi_i$ .

Next, the vibrational level density, belonging to  $S_0^{**}$  in the vicinity of the initial level  $\varphi_0$  was investigated using a direct count algorithm, which was designed in such a way as to select from the entire available density only those levels  $\varphi_i$  whose coupling  $V_{0i}$  to  $\varphi_0$  exceeded a given value  $W$ . The density  $\rho(W)$  thus obtained is the density of levels, interacting with  $\varphi_0$  through matrix elements greater than  $W$ . By repeating the computation at varying  $W$  we obtained dependences of  $\rho$  on  $W$ .

Figure 2 presents a computed dependence of  $\rho(W)$  on  $W$  at the following parameter values:  $\varphi_0$  corresponds to 3 quanta of  $\nu_4 = 136 \text{ cm}^{-1}$  ( $n_4 = 3$ );  $Q_0 = 1.5$  for all modes (both local and normal);  $\omega x = 2 \text{ cm}^{-1}$  (anharmonism of local modes for both Cr–O and Cr–Cl stretches);  $K = (\nu'/\nu'')^{\frac{1}{2}} = 0.85$  (for all local modes).

A decay process can take place only when  $\rho(W) \cdot W > 1$ . Therefore in the lower part of the figure the dependence of  $\rho(W) \cdot W$  on  $W$  is also displayed. For the considered case from figure 2 (lower part) we may tentatively conclude that  $\rho(W) \cdot W > 1$  for  $W > 0.0002 \text{ cm}^{-1}$ . This value of  $W$  corresponds to  $\rho(W) \approx 5000 \text{ l/cm}^{-1}$ . On the basis of these values we may use the Fermi golden rule to estimate the IC rate constant:  $K_{\text{IC}} = (2\pi/\hbar) \cdot V^2 \cdot \rho \approx 1.2 \times 10^{12} V^2 \cdot \rho \approx 2.4 \times 10^8 \text{ s}^{-1}$ . The obtained value is very similar to that derived from experimental data:  $K_{\text{IC}} = 1.8 \times 10^8 \text{ s}^{-1}$  (table 1). Thus at  $\varphi_0(n_4 = 3)$  we find out that the considered IC process involves an effective vibronic level density of  $\approx 5000 \text{ l/cm}^{-1}$ , while the total vibronic level density has been estimated to be  $\approx 5 \times 10^6 \text{ l/cm}^{-1}$ .

## 6. Dependence of relaxation rate constants on $n'_4$

The results of table 1 point to an increase of  $K_{IC}$  with  $n'_4$ . To verify whether this is consistent with our model description we have computed the dependence  $\rho(W)$  for  $n'_4 = 0$  which is also plotted in figure 2 for comparison. Indeed it is seen from the figure that the effective density at  $n'_4 = 3$  substantially exceeds that at  $n'_4 = 0$  which should definitely lead to enhancement of  $K_{IC}$  with  $n'_4$ . From the table it is seen that with the increase of  $n'_4$ ,  $K_{IVR}$  grows more steeply than  $K_{IC}$  and at  $n'_4 > 3$   $K_{IVR}$  dominates over  $K_{IC}$ . This behavior of  $K_{IVR}$  with  $n'_4$  remains to be analyzed.

## 7. Implications to multiphoton chemistry

A point of major interest is the vibrational characterization of the sparse set  $\varphi_i$ . The counting algorithm applied has yielded an average content of 12 Cr–O stretch quanta for each level from the estimated density of  $\approx 5000$  l/cm<sup>-1</sup>. This means that the sparse level density  $\rho$  is characterized by highly nonequilibrium distribution of vibrational excitation – extremely high average excitation of Cr–O stretch vibrational motion (about 12,000 cm<sup>-1</sup> from the total energy of these levels – 17,656 cm<sup>-1</sup>). The  $\{\varphi_i\}$  levels get populated on a time scale of  $\tau_{IC} = K_{IC}^{-1}$ . The levels decay subsequently (through IVR) into the total vibrational level density ( $5 \cdot 10^6$  l/cm<sup>-1</sup>), their energy being equilibrated among all molecular vibrational modes on a time scale  $\tau_{IVR} = K_{IVR}^{-1}$ . The time differentiation between these two processes (IC and IVR) is better at lower excess vibrational energy ( $n'_4 > 4$ , where  $K_{IC} > K_{IVR}$  (table 1)). Thus in the time range  $\tau_{IC} < t < \tau_{IVR}$  in the sparse manifold a predominant excitation of Cr–O vibrational motion persists.

Considering the “hot molecule” mechanism (Nakashima *et al* 1989) – absorption of a second UV photon from the highly vibrationally excited  $S_0^{**}$  state and subsequent dissociation: if the delay time of the second photon is in the time range  $\tau_{IC} < t < \tau_{IVR}$  a mode selective effect might be achieved. Such a procedure might lead to enhancement of Cr–O bond fission, while conventional photolysis results in Cr–Cl bond breaking (Halonbrenner *et al* 1968).

## References

- Halonbrenner P, Huber J R, Wild U and Gunthard H H 1968 *J. Phys. Chem.* **72** 3929  
Henry B R 1977 *Acc. Chem. Res.* **10** 207  
Lahmani F, Tramer A and Tric C 1974 *J. Chem. Phys.* **60** 4431  
McDonald J R 1975 *Chem. Phys.* **9** 423  
Nakashima N and Yoshihara K 1989 *J. Phys. Chem.* **93** 7763  
Rashev S 1991 *J. Chem. Phys.* (submitted for publication)  
Tinti D S, Baskin J S and Zewail A H 1989 *Chem. Phys. Lett.* **155** 243